

EMISSION OF MOLECULAR IONS FROM A PEPTIDE SAMPLE UNDER  $^{32}\text{S}$  BOMBARDMENT AT ENERGIES 25-90 MeV

F. RIGGI<sup>\*,\*\*\*</sup>, M.T. SANTANGELO<sup>\*</sup>, R.M. SPINA<sup>\*</sup>, M. LATTUADA<sup>\*\*,\*\*\*</sup> and C. SPITALERI<sup>\*\*,\*\*\*\*</sup>

<sup>\*</sup>Istituto Nazionale di Fisica Nucleare, Sezione di Catania Corso Italia 57, I-95129 Catania, Italy

<sup>\*\*</sup>Istituto Nazionale di Fisica Nucleare, Laboratorio Nazionale del Sud, Vl. A.Doria ang.S.Sofia, I-95100 Catania, Italy

<sup>\*\*\*</sup>and Dipartimento di Fisica, Università di Catania

<sup>\*\*\*\*</sup>and Istituto di Fisica, Università di Catania

Résumé- L'émission ionique secondaire a été étudié à partir de films minces solides avec un faisceaux de  $^{32}\text{S}$  à énergie entre 23 et 90 MeV. Les ions secondaire ont été identifié avec un système temps de vol. Le rendement d'émission ionique a été comparé avec différent modèles.

Abstract- The emission of different secondary ions from a dipeptide sample has been investigated under bombardment with  $^{32}\text{S}$  ions at energies 23-90 MeV. Desorbed ions were identified in a time-of-flight mass spectrometer. Yield curves were compared with different desorption models.

## 1. INTRODUCTION

Heavy ions with energies around 1 MeV/A have been used in several experiments on desorption of secondary ions from thin solid films /1-10/. The main aim of these studies was the investigation of the desorption mechanism under high energy heavy ion bombardment. For this reason the yields of different secondary ions from organic compounds (as well as from metallic surfaces) have been measured as a function of the primary ion parameters, such as mass, energy, charge state and angle of incidence. The energy range usually investigated covers the region where the maximum of the stopping power is expected for that particular projectile-target combination. Though the phenomenon is related in some way to the energy loss of the incoming ions in the electronic regime, the details of the desorption process are still a matter of interest. A comparison between the different proposed models requires the availability of experimental data in a wider range of the primary ion parameters.

In the present study the emission of different secondary ions from a dipeptide sample has been investigated by using a  $^{32}\text{S}$  beam from the LNS Tandem accelerator. The investigated energy range was from 23 to 90 MeV, roughly corresponding to 0.7-3 MeV/A. Secondary ions desorbed from the sample were identified in a time-of-flight mass spectrometer recently built for desorption studies /11/. The measured yields were compared with different models.

## 2. EXPERIMENTAL METHOD

The experiment was performed at the LNS Tandem Laboratory by using a  $^{32}\text{S}$  beam. The beam was scattered at  $22^\circ$  in a thin  $^{197}\text{Au}$  target to reduce

intensity to a suitable level. Scattered  $^{32}\text{S}$  ions were allowed to pass through a collimator and the sample and are detected by a solid state counter giving energy and timing signals. The desorbed ions are accelerated to 5 keV by a 90% transmission grid placed at 3 mm from the sample and then allowed to drift in a field-free region (length 200 mm) before being stopped in a microchannel-plate (MCP) detector. Fig.1 shows the lay-out of the experimental apparatus.

Fast signals from the solid state and MCP detector are sent through constant fraction discriminators (CFD) to the start and stop inputs of a multistop time-to-digital converter. Thresholds on the CFD's are adjusted to select only the elastic scattered ions in the solid state counter and to

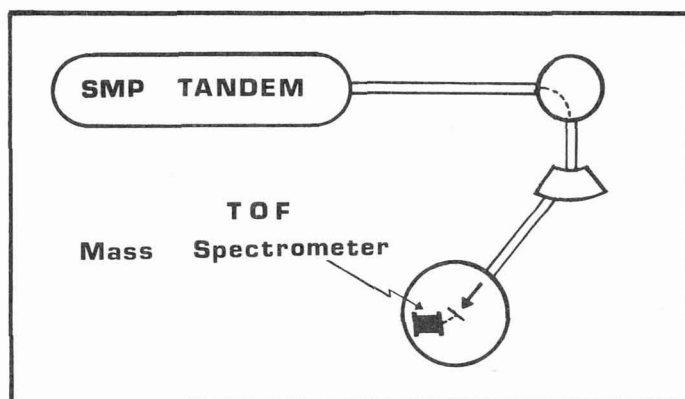


Fig.1 - Schematic lay-out of the experimental apparatus.

optimize the signal-to-noise ratio in the MCP detector.

The sample used in the present experiment was a dipeptide (Alanine-Alanine, mol. weight 160) which was electrosprayed /12-13/ on a 2  $\mu\text{m}$  aluminised polyester foil from a 0.5  $\mu\text{g}/\mu\text{L}$  solution in Methanol.

Vacuum in the scattering chamber used in this investigation was obtained through a turbomolecular pump. Pressure was  $10^{**}(-6)$  mbar throughout all measurements.

Time spectra were collected by using an IBM/XT personal computer for on-line acquisition and analysis. Mass peaks over the entire time-of-flight range were identified through calibration over known peaks. Mass resolution in the present experiment was estimated to be around  $M/\delta M=250$ , which was adequate for the expected molecular ions from the Ala-Ala sample. Absolute efficiency of the spectrometer is not easy to determine, since it depends also on many electrostatic and geometrical factors /14-15/. Sample coverage of the surface influences also the absolute yields. For these reasons only relative yields (i.e. number of detected secondary ions divided by the number of elastic scattered  $^{32}\text{S}$  ions) are reported. Reproducibility of the results was checked by measuring the yields at the same energy after a few hours. The  $\text{H}^+$  yields were found to be the same within 1%.

### 3. RESULTS AND DISCUSSION

Fig.2 shows the structure of the Ala-Ala molecule and the mass assignment

to some observed positive ion peaks from Ala-Ala. Nomenclature for sequence ions was taken from ref./16/. Positive ion time-of-flight spectra were collected at several  $^{32}\text{S}$  incident energies between 36 and 100 MeV. Taking into account the kinematical factor due to the scattering in the Au target and the energy loss in the backing foil, the effective  $^{32}\text{S}$  energies range between 23 and 90 MeV. Fig.3 shows a TOF spectrum of Ala-Ala obtained in the present experiment. The width of the  $\text{H}^+$  peak is around 2 ns. The inset reports the molecular ion region, showing the largest peaks at masses 183 and 205, corresponding to  $(\text{M}+\text{Na})^+$  and  $(\text{M}+2\text{Na}-\text{H})^+$ .

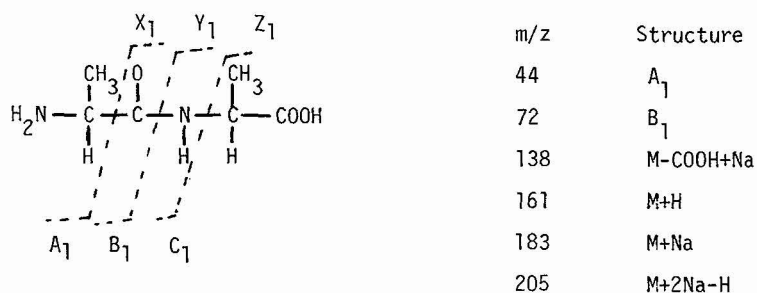


Fig.2 - The Ala-Ala molecule investigated in the present experiment and a mass assignment to positive ion peaks in the TOF spectra.

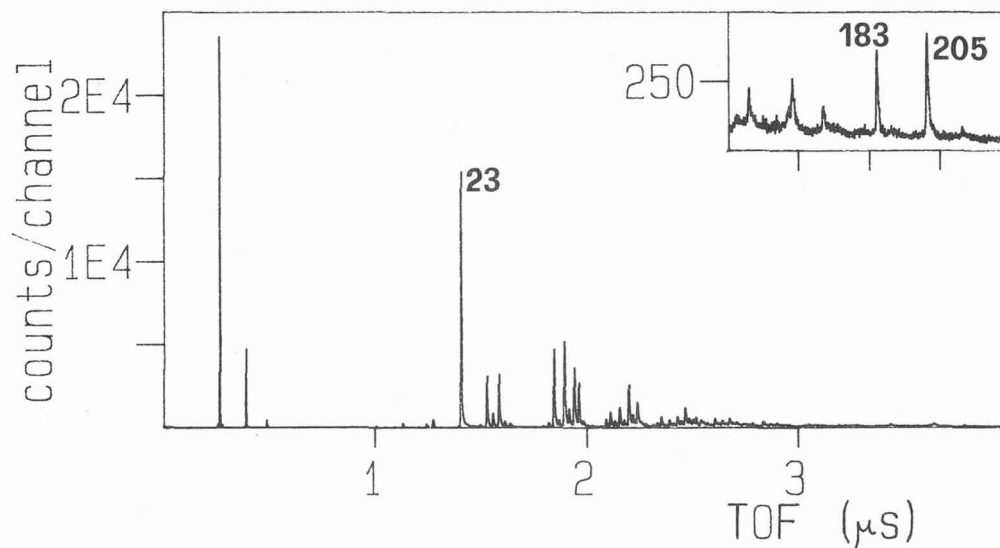


Fig.3 - Time-of-flight spectrum of the Ala-Ala sample. Primary ions:  $^{32}\text{S}$  beam at  $E=23$  MeV.

Different behaviours were found for the yield curves, which could be indicative of different desorption mechanisms.

Fig.4 shows the measured yields of the lightest peaks  $H^+$ ,  $H_2^+$ ,  $H_3^+$  as a function of the effective primary ion energy. Since desorption occurs at the exit side of the sample, the measured yields refer to charge-equilibrated distribution of the primary ions. It is usual to compare desorption yields with some function of the electronic stopping power, since this gives a simple way of estimating the energy transferred to the sample molecules. This was done for the data reported in fig.4, by using Northcliffe and Schilling tables /17/. The shape of the yield curves are well fitted by a  $(dE/dx)^2$  behaviour, especially for  $H_2^+$  and  $H_3^+$ . A  $(dE/dx)^2$  trend has been found also for other ions /1,4,6,10/.

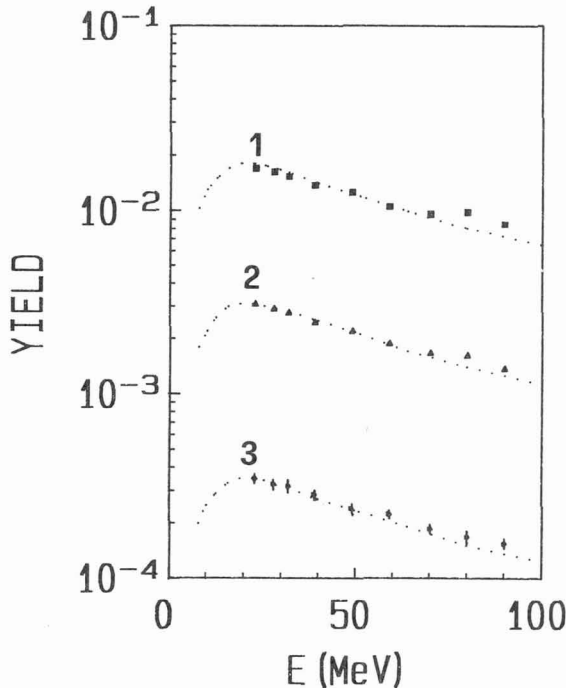


Fig.4 - Yield curves of  $H^+$ ,  $H_2^+$ ,  $H_3^+$  as a function of the energy of the primary ions. Dotted lines show the  $(dE/dx)^2$  shape.

Other model have been proposed by different authors, by considering different contributions to the total energy loss of the incoming ions. Two cases were considered by the Caltech group /18/, by assuming that within a cylinder of radius  $r_0$  around the projectile path the atoms form a hot plasma in thermal equilibrium with an initial temperature  $T_0$ . At constant temperature this gives yields which are proportional to the fourth power of the primary ionization rate, i.e.  $Y = A (dJ/dx)^4$ , where  $dJ/dx = (Zff/v)^2 \lg(E/B)$ . The previous equation gives a realistic fit to the data in fig.4 in the high energy part of the yield curve but underestimates the yield at low energy, where a maximum is expected around 30 MeV.

Realistic shapes were also obtained through the simple parametrization  $Y(E) = \sum_i w_i q_i^2/E$ , where the  $w_i$  are the weights of the different charge states. Fig.5 shows the yield curves for different mass peaks. A different shape is observed for the yield of mass peaks arising from impurities. Two of them are shown in fig.5, corresponding to masses 41 and 57. These shapes are clearly not fitted neither by a  $(dE/dx)^2$  nor by a  $(dJ/dx)^4$  shape.

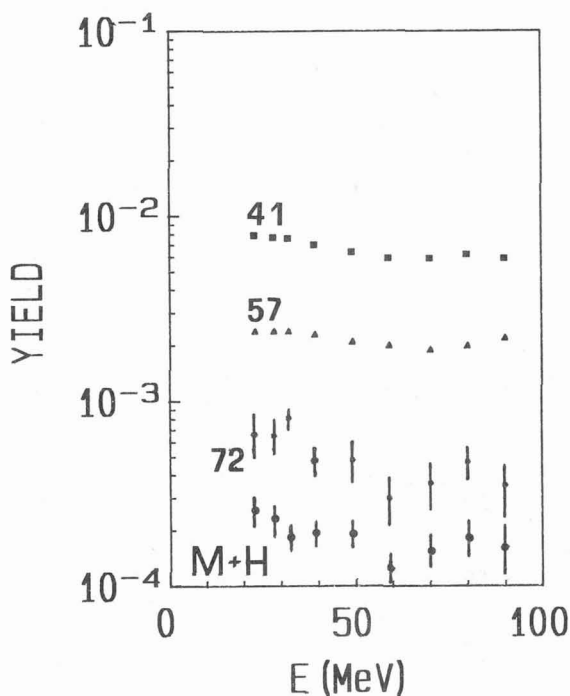


Fig.5 - Yield curves of masses 41, 57, 72 (fragment B<sub>1</sub>), 161 (M+H) as a function of the energy of the primary <sup>32</sup>S ions.

Energy trend with a low value of the slope were already observed for desorption induced by <sup>32</sup>S ions /6/, whereas the corresponding slopes for 16O- and 19F-induced desorption were larger.

Mass peaks which come from the Ala-Ala sample give yield curves which show large fluctuations. Fig.5 shows also typical patterns corresponding to mass 72 (fragment B, see fig.2) and 161 (M+H). The same pattern was found also for other peaks, such as 44<sup>+</sup> and 183<sup>+</sup>, even when the associated errors are lower than those reported for the 72<sup>+</sup> and 161<sup>+</sup> data. Possible systematic errors associated with mass-dependent detection efficiency can be excluded since completely different behaviours were observed for peaks having similar mass, like 41<sup>+</sup> and 44<sup>+</sup>. It cannot be excluded however that these patterns could arise from different, correlated experimental effects. Further investigation could help to understand whether the energy dependence of the yield curves for the molecular fragments could show some non monotonic behaviour in this energy region.

In conclusion, the study of secondary ion emission from complex molecules under bombardment with heavy ions in a wide energy range could provide useful information on the desorption mechanism, since i) different theoretical models could be better tested at high energy, while giving comparable results at low energy; ii) different desorption mechanisms could show up for different fragments and/or molecular ions; iii) some evidence (if any) for fragment-dependent energy trends of the desorption yields could be searched for.

## REFERENCES

- /1/ HAKANSSON, P. and SUNDQVIST, B., Rad.Eff.61(1982)179.
- /2/ BECKER, O., DELLA-NEGRA, S., LE BEYEC, Y. and WIEN, K., Nucl.Instr.Me-  
thods B16(1986)321.
- /3/ VOIT, H., FROHLICH, H., DUCK, P., NEES, B., NIESCHLER, E., BISCHOF, W.,  
and TIERETH, W., IEEE Trans. Nucl.Sci. Ns-30(1983)1759.
- /4/ HAKANSSON, P., KAMENSKY, I. and SUNDQVIST, B., Nucl.Instr.Methods  
198(1982)43.
- /5/ VOIT, H., NEES, B., NIESCHLER, E. and FROHLICH, H., Int.J.Mass Spe-  
ctrom.Ion Phys. 53(1983)201.
- /6/ DUCK, P., FROHLICH, H., TREU, W. and VOIT, H., Nucl.Instr.Methods  
191(1981)245.
- /7/ DUCK, P., TREU, W., FROHLICH, H., GALSTER, W. and VOIT, H., Surf.Sci.  
95(1980)603.
- /8/ NEES, B., NIESCHLER, E., BISCHOF, N., DUCK, P., FROHLICH, H., TIERETH,  
W. and VOIT, H., Surf.Sci.145(1984)197.
- /9/ NEES, B., NIESCHLER, E., BISCHOF, N. DUCK, P., FROHLICH, H., TIERETH,  
W. and VOIT, H., Rad.Eff. 77(1983)89.
- /10/ DELLA-NEGRA, S., JACQUET, D., LORTHIOIS, J., LE BEYEC, Y., BECKER, O.  
and WIEN, K., Int.J.Mass Spectrom.Ion Phys. 53(1983)215.
- /11/ RIGGI, F. and SPINA, R.M., N.Cimento D(1988), in press.
- /12/ MC NEAL, C., MAC FARLANE, R.D. and THURSTON, E., Anal.  
Chem.51(1979)2037.
- /13/ RIGGI, F. and SPINA, R.M., INFN Report TC-88/3.
- /14/ RIGGI, F., Nucl.Instr.Methods B22(1987)588.
- /15/ RIGGI, F., Nucl.Instr.Methods B31(1988)588.
- /16/ ROEPSTOFF, P., Biomed.Mass Spectrom. 11(1984)601.
- /17/ NORTHCLIFF, L.C., and SHILLING, R.F., Nucl.Data Tables A7(1970)273.
- /18/ SEIBERLING, L.E., GRIFFITH, J.E. and TOMBRELLO, T.A., Rad.  
Eff.52(1980)201.